PCCP

Accepted Manuscript

ROYAL SOCIETY OF CHEMISTRY

www.rsc.org/pccp

Three distinct open-pore morphologies from a single particle-filled polymer blend

Trystan Domenech, Junyi Yang, Samantha Heidlebaugh, Sachin S. Velankar[*]*, Dept. of Chemical Engineering, University of Pittsburgh, Pittsburgh PA 15261, USA.*
Phone: (+1) 412-624-9984 ; Email: velankar@pitt.edu

Abstract

Ternary mixtures composed of polyisobutylene (PIB), polyethylene oxide (PEO), and silica particles yield three distinct open-pore morphologies depending on mixture composition: (1) *pendular network* (particles bonded together by menisci of PEO); (2) *capillary aggregate network* (particles and PEO form a combined phase with strongly solid-like properties which percolates); (3) *cocontinuous morphology* (silica and the PEO form a highly viscous combined phase which retards interfacial tension-driven coarsening). Remarkably, interfacial tension plays altogether different roles in stabilizing these three morphologies: stabilizing the first, not affecting the second, and destabilizing the last. The first two of these morphologies appear to be generalizable to other systems, e.g. to oil/water/particle mixtures. In all three cases, the pores do not collapse even after flow, i.e. all three porous morphologies are amenable to processing.

Keywords: rheology; suspension; porous; percolation; ternary mixtures

Introduction

Open pore structures are useful in a wide variety of applications, e.g. absorbing and retaining fluids (e.g. wound dressing, personal hygiene, oil spill absorption), highly compliance structures (e.g. seat cushions), providing percolating pathways (conductive electrodes, battery separator materials, filters, tissue engineering scaffolds). Topologically, open pore structures have two interpenetrating continuous phases, one of which is regarded as "pores" (i.e. typically filled with air or with water), and the other phase being a solid with some mechanical integrity. Open pore structures have diverse morphologies such as networks composed of slim struts (e.g. open-celled foams[1]), interconnected cavities (e.g. polymerized high-internal phase emulsions[2-5]), interstitial spaces between fused particles (e.g. sintered powders[6]) or between fiber mats[7-8], or smooth bicontinuous phases[9-10]. Here we show that a single system composed of two immiscible polymers and one particulate species yields three distinct open-pore morphologies depending on the composition of the mixture.

Experimental

The experimental system is composed of silica particles, and two immiscible polymers, polyethylene oxide (PEO) and polyisobutylene (PIB). Details of the materials are provided in Table 1. All components were mixed together (next paragraph) at 80℃, a temperature at which the PEO and PIB have similar viscosities. Upon cooling to room temperature, the PEO crystallizes into a semicrystalline solid (melting point 65℃); this provides a facile means of quenching the morphology developed under melt-blending conditions. The continuous phase PIB was extracted in octane, leaving behind the consolidated masses of the PEO and the particles discussed below. These were fractured, coated with palladium, and imaged by scanning electron microscopy (SEM).

Being composed of molten polymers, these samples have viscosities far higher than oil/water mixtures. Accordingly they cannot be mixed by simple shaking or by equipment such as a homogenizer. Therefore samples were mixed in a custom-built polymer mixer comprising a rotating disc-cup assembly of 5 ml volume. Three ball bearings were added between the rotating disc and the cup to ensure intensive mixing[11-13]. The cup was maintained at 80℃ using an electric heater. All samples were mixed identically: the minority polymer PEO was first dispersed into the PIB at 1200 rpm, particles were added, and mixing continued for an additional 5 min. Samples were cooled in air immediately after mixing, followed by 30 minutes at ~4℃ to ensure complete crystallization of the PEO.

Results and Discussion

The six different compositions discussed in this article can be placed in a ternary composition diagram[14-15], Fig. S1, from which the volume fractions of all three species can be read off. However for this article, it is more convenient to specify the composition in terms of two parameters: the particle volume fraction, ϕ_p and $\varrho = \phi_{PEO}/\phi_p$, which is the wetting fluid loading relative to the particle loading. This representation is shown in Fig. 1A. Of the six compositions discussed, the three with high values of ϕ_p yield three distinct types of open-pore structures illustrated schematically in Fig. 1B, and discussed below.

Fig. 2A illustrates the first kind of porous structure, dubbed a *pendular network*. This appears when the PEO loading is substantially lower than particle loading, i.e. ϱ is on the order of 0.1, and no larger than 0.3. In this range of ϱ, when the sample is well-mixed, the wetting fluid forms pendular menisci that connect the particles into aggregates. If ϕ_p is small, the pendular aggregates are discrete (Fig. S2). With increasing ϕ_p (at fixed ϱ), these aggregates grow until they percolate, and a pendular network results. Previously we showed that the percolation threshold is only a few percent[12], i.e. the ϕ_p of Fig. 2A far

exceeds the percolation threshold. This pendular network structure is analogous to wet sand in which the sand particles are bridged by menisci of water[16].

Fig. 2B illustrates the second kind of porous structure dubbed a *capillary aggregate network*, which appears when ϱ is 0.5-1. Since the particles are fully-wetted by the PEO, and since the PEO fraction is comparable to the particle fraction, the PEO engulfs the particles completely to form a combined phase. This combined phase is highly concentrated with an internal particle volume fraction of $\phi_p^{combined} = \frac{\phi_p}{\phi_p+\phi_{PEO}} = (1+\varrho)^{-1}$. The dependence of $\phi_p^{combined}$ on ϱ is illustrated in Fig. 3A. For instance, for Fig. 2B, $\varrho = 0.9$, which corresponds to $\phi_p^{combined} = 0.53$. Due to this high particle loading, this combined phase is expected to resemble a paste with solid-like rheological properties. We sought to measure the rheology directly by preparing a particle-in-PEO suspension (no PIB added) at a particle loading of 53 vol%. However we were unsuccessful since the extremely solid-like rheology makes homogeneous mixing difficult. We were however able to prepare particle-in-PEO suspensions with somewhat lower particle loadings and Fig. S4 shows the Large Amplitude Oscillatory Shear (LAOS) rheology of some samples measured at a frequency of 10 rad/s. At 40 vol% particles, G'' exceeds G' over the entire amplitude range, indicative of liquid-like behavior. In contrast at 44 and 50% particles, the rheological behavior is typical of paste-like materials: at low amplitude $G' > G''$, whereas at some larger amplitude, there is a crossover which is often regarded as a signature of yielding. From these data, one may extract the linear viscoelastic moduli of these suspensions (Fig. 3B), and by interpolation, conclude that samples with over ~42% particles have $G' > G''$ indicative solid-like rheology. Thus, a suspension with 53% particles (corresponding to the PEO-phase in Fig. 2B) would be strongly solid-like. Accordingly, when the ternary blend of Fig. 2B is subjected to intense mixing, the combined phase tends to form misshapen "blobs" called *capillary aggregates*[17]. Capillary aggregates tend to be non-spherical since their internal yield stress exceeds their capillary pressure, thus interfacial tension cannot induce a misshapen aggregate to relax into a spherical shape. At low values of ϕ_p these blobs are discrete (Fig. S3), however with increasing ϕ_p, they percolate into the network of Fig. 2B. This network is composed of roughly spherical capillary aggregates which are bonded together through relatively narrow necks[12]. This phenomenon has been documented previously in mixtures of oil, water, and fat where it was called *partial coalescence*[18]. A more evocative term coined by Caggioni et al. is *anisotropic endoskeletal drops*[19], i.e. drops with an internal network that sustains non-spherical shapes. We note that the particles in these previous papers were needle-like crystals[18-19], and hence could develop a yield stress at even low particle loadings. Here, the particles are spherical, and hence anisotropic drop shapes can survive only at high $\phi_p^{combined}$ (low ϱ)

values. Incidentally, the fact that capillary aggregates form at certain compositions is not new[17]; what is unusual is that the capillary aggregates join together into a percolating network.

The third type of porous structure, dubbed a *cocontinuous morphology* (Fig. 2C) is evident at $\varrho = 1.75$. The particles and the PEO still form a combined phase, but now the combined phase is much less crowded than in Fig. 2B. For example, for Fig. 2C, Fig 3A suggests that at $\varrho = 1.75$, the particle volume fraction in the combined phase is 0.36. At this particle loading, the combined phase is highly viscous, but it no longer has significant solid-like properties (indeed even at 40% particles, Fig. S4 indicates liquid-like rheology). Accordingly, particles no longer protrude out from the PEO phase, instead the liquid/liquid interface appears smooth, as typical of systems in which capillarity dominates. Under these conditions, if the combined phase is dilute (Fig. S5), the morphology is composed of spherical drops of PEO with particles incorporated inside. In Fig. 2C in contrast, the combined phase loading is $(\phi_p + \phi_{PEO}) = 0.55$, and a cocontinuous morphology is obtained. Given sufficient time under quiescent conditions after mixing, this system would coarsen indefinitely, and eventually the cocontinuous structure would be destroyed by gravity (there is a significant density difference between the phases due to the high density of silica). Yet, due to the high internal viscosity of the combined phase, coarsening and collapse are relatively slow processes. Thus even air-cooling is sufficiently rapid that the crystallization of PEO can quench the cocontinuous structure readily. It is crucial to note that the particle-free PEO/PIB blends do not form cocontinuous morphologies at *any* PEO:PIB ratio. We have prepared particle-free PEO/PIB blends across a range of compositions and in all cases, the morphology is either a PEO-in-PIB with spherical PEO drops, or vice versa[20]. Thus, the particles are essential to stabilize the cocontinuous morphology. We surmise that the mechanism for such stabilization resembles viscoelastic phase separation[21]: since the combined PEO+particles phase has a high viscosity, interfacial coarsening and breakup, which usually destroy a cocontinuous morhology, are greatly retarded. Incidentally we note that cocontinuous morphologies are commonly reported in the polymer blends literature, even in the absence of particles[9]. In those cases, the polymers being blended have viscosities that are typically 2-3 orders of magnitude higher than those used here. Due to those high viscosities, the morphologies can be quenched readily by cooling.

It is important to note explicitly the major differences between the three morphologies. The pendular network is inherently a particle-scale structure, with the capillary force playing the role of a pair-wise attraction between particles. The percolating network is built from the individual particles bonded together by capillary menisci[16]. The immediate implication is that the pore size is comparable to the particle size, i.e. as long as the network is homogeneous, pore size can be changed only by changing the particle size. In contrast, the capillary aggregate network uses as building blocks not individual particles,

but aggregates comprising a large number of particles, together engulfed by the wetting fluid. Thus the pore size is decoupled from the particle size, and is instead set by the composition (which determines the rheology of the combined particle+PEO phase) and by the mixing conditions (which determines the size of largest capillary aggregate that can survive the mixing process). Finally the pore size of cocontinuous morphology is also decoupled from the particle size. But unlike in capillary aggregates, the combined phase is not internally jammed, and its rheological behavior is liquid-like. Thus this morphology is unstable, and unlike the previous two morphologies, quenching is essential to suppress morphological coarsening. In the present case, quenching is provided by crystallization of PEO, but one may also arrest coarsening by gelation, vitrification, or crosslinking of one or both phases. Since the cocontinuous morphology results from a competition between viscous stress and interfacial tension, we anticipate that the size-scale of the morphology would reduce if the mixing speed were increased although we have not tested this.

It is interesting to note that capillarity (in the sense of minimizing the liquid-liquid interfacial area) plays completely different – indeed opposing – roles in these three cases. In the pendular network, the pairwise attractive force between the particles is attributable to interfacial tension (indeed the meniscus force is proportional to interfacial tension)[22]. Thus the stability of the particle network depends primarily on capillarity; any additional interparticle attractions would confer additional stability. In contrast, the capillary aggregate network is stabilized primarily by the solid-like rheology of the combined particle+PEO phase, and to a first approximation, the stability does not rely on capillarity. In a previous article on oil/water/particle systems[15], we have argued that since particles protrude out of the surface of the capillary aggregates, the liquid/liquid interface has negative curvature, and hence "pulls together" the particles with a Laplace pressure that is on the order of (surface tension)/(particle size). This Laplace pressure increases the interparticle friction forces, and may therefore increase the yield stress within the capillary aggregates. To the extent that this mechanism is active, capillarity may have a stabilizing effect on the capillary aggregate network. Finally, in the cocontinuous morphology, capillarity induces morphological coarsening as well as breakup into a droplet-matrix morphology. Thus in this case, capillarity has a *de*stabilizing effect. It is for this reason that the cocontinuous structure *must* be quenched, whereas the pendular or capillary aggregate networks need not be.

It is of immediate interest to ask whether these three morphologies are unique to polymeric mixtures, or if they may be realized even when the fluids are oil and water. The pendular network is highly general and can be realized in almost any particulate system in which the particles are preferentially-wetted by the minority phase. For instance, Fig. S6 illustrates a pendular network realized from large glass particles, but using oil as the continuous phase and water as the dispersed phase that forms the meniscus. With

hydrophobic particles, one may also realize an inverted structure in which water is continuous and oil is the meniscus-forming phase. The capillary aggregate network also appears to be generalizable to oil/water systems. For instance, Figs. S7A&B show a network formed by using the same particles as used in the rest of this paper, but with oil and water as the two fluids. The sample was mixed using a high speed rotor-stator mixer using the procedure described in the caption to Fig. S7. A network of capillary aggregates is clearly evident at $\varrho = 0.75$. The same procedure was applied using polyethylene particles, methanol and a small quantity of mineral oil (see caption of Fig. S8 for compositions). Since the polyethylene particles are highly oleophilic, a capillary aggregate network with methanol as the continuous phase was realized. Finally, we were unsuccessful in realizing cocontinuous morphologies from oil/water systems. For instance, Fig. S7A&B show capillary aggregates realized in an oil/water system at $\varrho = 0.75$. Upon increasing the ϱ to 0.8, the capillary aggregates become capable of complete coalescence indicative of increasingly liquid-like behavior of the (silica+water) combined phase. But instead of realizing a cocontinuous morphology, Fig. S7C shows that the system collapses into separated mixture of oil and (silica+water). Thus even if the cocontinous morphology was present during mixing, it does not survive for any significant duration after mixing. We believe that this rapid collapse is attributable to the much lower fluid viscosity of the oil/water system as compared to the PEO/PIB blends. Thus, as already emphasized above, the cocontinuous morphology can be realized only if at least one of the fluid phases can be solidified rapidly. In summary, at least two of the three morphologies appear to be generalizable to oil/water systems; whereas the last, the cocontinuous structure, is not.

We have not investigated in detail the boundaries separating these three porous structures. A review across a wide range of systems suggests that the pendular aggregate morphology becomes unstable when menisci binding different particles start coalescing together[14]. This happens at $\rho \sim 0.35 - 0.5$, which may be taken as the boundary separating a pendular network from capillary aggregate network. The boundary between capillary aggregates and cocontinuity (if cocontinuity is realized) depends on the ϱ value above which the combined phase has liquid-like rheology. This boundary is more difficult to generalize across a wide range of systems; depending on the nature of particle interactions, some combined phases may become solid-like at even relatively high ϱ values. Indeed, some previous researchers have reported stabilization of cocontinuous-like morphologies in polymeric systems even at very low particle loading[23-25] because the nanoparticles were able to induce solid-like rheology even at low particle loading.

Conclusions and Outlook

In summary, we show that by changing composition, a single three-component mixture yields three porous morphologies that have distinct size-scale and entirely different mechanisms of structural

stabilization. What is most remarkable is interfacial tension plays an altogether different role, stabilizing the pendular morphology, destabilizing the cocontinuous morphology, and (to a first approximation) not affecting the capillary aggregate network. At least two of these porous structures appear to be generalizable to other mixtures, including to oil/water/particle mixtures. Two noteworthy aspects that are relevant to practical applications must be emphasized. First, in all three of the porous structures reported here, both phases are continuous, i.e. they may be regarded as open-pore structures with potential applications listed in the first paragraph of this article. The resulting porous structures may be used directly, e.g. for tissue scaffolds. Alternately, one may remove the non-wetting fluid by selective extraction (as done here), drying, or simply draining out the fluid, and then undertake further modifications, e.g. particle sintering, back-filling the pores with other fluids, etc. Indeed particulate networks based on capillary attractions have already been used to fabricate porous ceramics[26-27]. Second, all three of these structures were generated under flow conditions, and longer flow duration under molten conditions does not disrupt them. Thus, as long as the yield stress is not too high (which may happen at higher particle loadings), these morphologies are all amenable to be molded, extruded, or injected – without losing their open pore morphology. This is in contrast to many other methods of fabricating similar open-cell porous structures, e.g. polymerizing a high internal phase emulsion, preparing a bijel precursor[10], leaching a porogen[28], phase separation of a polymer solution, or direct foaming of polyurethanes. In all those cases, open-celled porous structure cannot be subjected to flow, either because it is quenched, or because it does not survive under flow.

Acknowledgements: We gratefully acknowledge the National Science Foundation for financial support (NSF-CBET grant no. 0932901 and 1336311), Samantha Heidlebaugh (Figs. S6 and S7) and Dr. Manjulata Singh and Prof. Shilpa Sant (Figs. S6b) respectively. Fig. S1 was drawn using the ternary diagram template provided by Graham and Midgley[29].

References

1. Defonseka, C., *Practical Guide to Flexible Polyurethane Foams*. Smithers Rapra Technology: **2013**.
2. Haibach, K.; Menner, A.; Powell, R.; Bismarck, A., Tailoring mechanical properties of highly porous polymer foams: Silica particle reinforced polymer foams via emulsion templating. *Polymer* **2006,** *47* (13), 4513-4519.
3. Barbetta, A.; Rizzitelli, G.; Bedini, R.; Pecci, R.; Dentini, M., Porous gelatin hydrogels by gas-in-liquid foam templating. *Soft Matter* **2010,** *6* (8), 1785-1792.
4. Foudazi, R.; Gokun, P.; Feke, D. L.; Rowan, S. J.; Manas-Zloczower, I., Chemorheology of Poly(high internal phase emulsions). *Macromolecules* **2013,** *46* (13), 5393-5396.
5. Silverstein, M. S., Emulsion-templated porous polymers: A retrospective perspective. *Polymer* **2014,** *55* (1), 304-320.

6. Liu, P. S.; Chen, G. F., *Porous Materials: Processing and Applications*. Butterworth-Heineman: Oxford, **2014**.
7. Masoodi, R.; Pillai, K., *Wicking in Porous Materials: Traditional and Modern Modeling Approaches*. CRC Press: Boca Raton, **2013**.
8. Ding, B.; Yu, J., *Electrospun Nanofibers for Energy and Environmental Applications*. Springer: Heidelberg, **2014**.
9. Potschke, P.; Paul, D. R., Formation of Co-continuous structures in melt-mixed immiscible polymer blends. *J. Macromol. Sci.-Polym. Rev* **2003,** *C43* (1), 87-141.
10. Lee, M. N.; Mohraz, A., Bicontinuous Macroporous Materials from Bijel Templates. *Adv. Mat.* **2010,** *22* (43), 4836-4841.
11. Maric, M.; Macosko, C. W., Improving polymer blend dispersions in mini-mixers. *Polym. Eng. Sci.* **2001,** *41* (1), 118-130.
12. Domenech, T.; Velankar, S. S., On the rheology of pendular gels and morphological developments in paste-like ternary systems based on capillary attraction. *Soft Matter* **2015,** *11* (8), 1500-16.
13. Domenech, T.; Velankar, S., Capillary-driven percolating networks in ternary blends of immiscible polymers and silica particles. *Rheol. Acta* **2014,** *53* (8), 1-13.
14. Velankar, S. S., A non-equilibrium state diagram for liquid/fluid/particle mixtures. *Soft Matter* **2015,** *11* (43), 8393-8403.
15. Heidlebaugh, S. J.; Domenech, T.; Iasella, S. V.; Velankar, S. S., Aggregation and Separation in Ternary Particle/Oil/Water Systems with Fully Wettable Particles. *Langmuir* **2014,** *30* (1), 63-74.
16. Herminghaus, S., Dynamics of wet granular matter. *Adv. Phys.* **2005,** *54* (3), 221-261.
17. Pietsch, W., Chapter 7: Tumble/growth agglomeration. In *Agglomeration Processes: Phenomena, Technologies, Equipment*, Wiley: Weinheim, **2008**.
18. Boode, K.; Walstra, P., Partial Coalescence in Oil-in-Water Emulsions .1. Nature of the Aggregation. *Colloid Surf. A* **1993,** *81*, 121-137.
19. Caggioni, M.; Bayles, A. V.; Lenis, J.; Furst, E. M.; Spicer, P. T., Interfacial stability and shape change of anisotropic endoskeleton droplets. *Soft Matter* **2014,** *10* (38), 7647-7652.
20. Domenech, T.; Velankar, S. S., Microstructure and phase inversion in three phase polymer/polymer/particle blends. *In preparation.* **2015**.
21. Tanaka, H., Viscoelastic phase separation. *J. Phys.-Condes. Matter* **2000,** *12* (15), R207-R264.
22. Willet, C. D.; Johnson, S. A.; Adams, M. J.; Seville, J. P. K., Chapter 28: Pendular capillary bridges. In *Handbook of powder technology, Vol. 11, Granulation*, Salman, A. D.; Hounslow, M.; Seville, J. P. K., Eds. Elsevier: Amsterdam, **2007**.
23. Cai, X. X.; Li, B. P.; Pan, Y.; Wu, G. Z., Morphology evolution of immiscible polymer blends as directed by nanoparticle self-agglomeration. *Polymer* **2012,** *53* (1), 259-266.
24. Khademzadeh Yeganeh, J.; Goharpey, F.; Moghimi, E.; Petekidis, G.; Foudazi, R., Manipulating the kinetics and mechanism of phase separation in dynamically asymmetric LCST blends by nanoparticles. *PCCP* **2015,** *17* (41), 27446-27461.
25. Wu, G.; Li, B.; Jiang, J., Carbon black self-networking induced co-continuity of immiscible polymer blends. *Polymer* **2010,** *51* (9), 2077-2083.
26. Dittmann, J.; Koos, E.; Willenbacher, N., Ceramic Capillary Suspensions: Novel Processing Route for Macroporous Ceramic Materials. *J. Am. Ceramic Soc.* **2013,** *96* (2), 391-397.

27. Koos, E.; Willenbacher, N., Capillary Forces in Suspension Rheology. *Science* **2011,** *331* (6019), 897-900.
28. Tessmar, J. K. V.; Holland, T. A.; Mikos, A. G., Salt leaching for polymer scaffolds: Laboratory-scale manufacture of cell carriers. In *Scaffolding in tissue engineering*, Ma, P. X.; Elisseeff, J., Eds. CRC Press: Boca Raton, **2006**.
29. Graham, D. J.; Midgley, N. G., Graphical representation of particle shape using triangular diagrams: An Excel spreadsheet method. *Earth Surface Processes and Landforms* **2000,** *25* (13), 1473-1477.

Table 1

	viscosity (80°C)	**MW**	**Supplier**
polyethylene oxide (PEO)	13 Pa.s	20 kg/mol	Fluka
polyisobutylene (PIB)	8 Pa.s	2400 g/mol	Soltex
silica average ~2 μm diameter			Industrial Powder

List of figures

Fig. 1: (A) Compositions of the samples discussed in the article. The same compositions are represented within a ternary composition diagram in Fig. S1. (B) Idealized illustrations of the three different types of porous structures corresponding to the compositions indicated by the arrows.

Fig. 2: (A) Pendular network (B) Capillary aggregate network; (C) Cocontinuous morphology. Images in the lower row are the same samples as the upper row, but at higher magnification.

Fig. 3: (A): The function $\phi_p^{combined} = (1 + \varrho)^{-1}$, corresponding to the particle volume fraction in the PEO-phase of a PIB/PEO/particle blend. The three horizontal lines correspond to the ϱ values of the three porous structures of Fig. 2. (B) Linear viscoelastic moduli G' and G" of suspensions of particles in PEO.

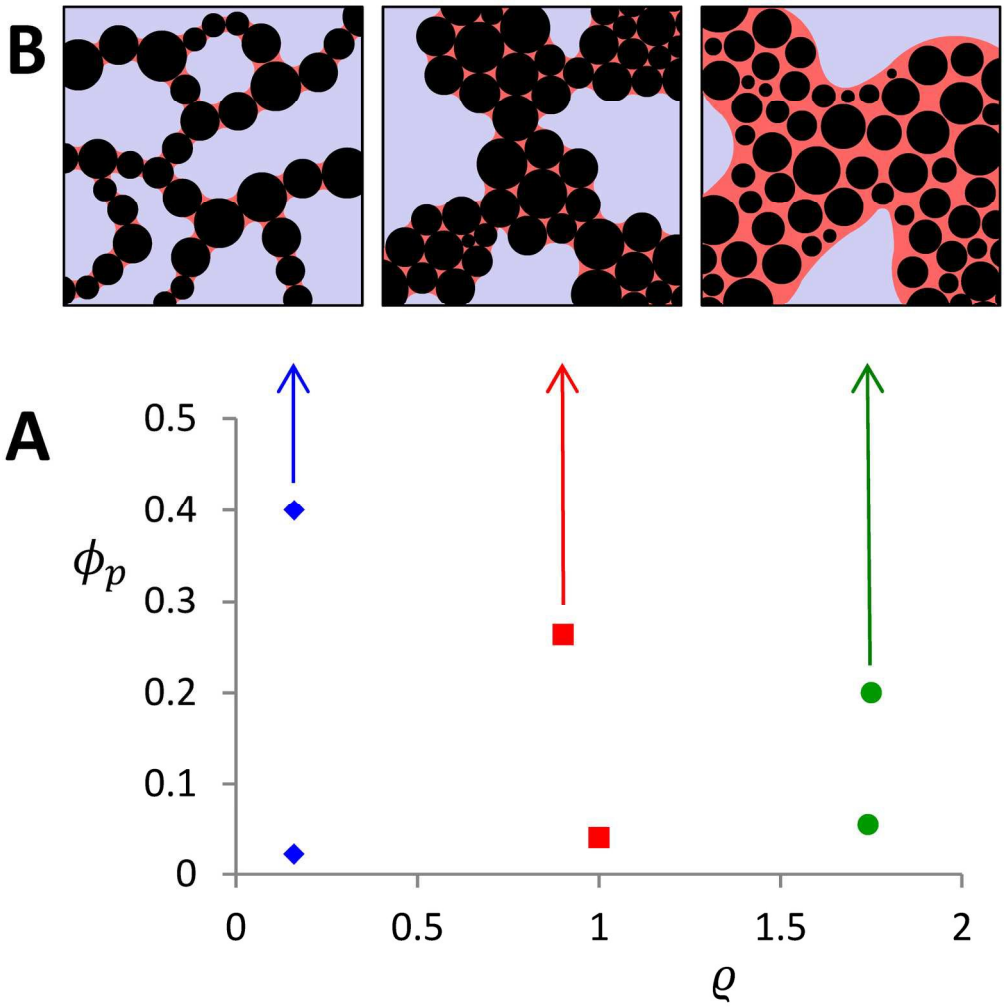

84x85mm (600 x 600 DPI)

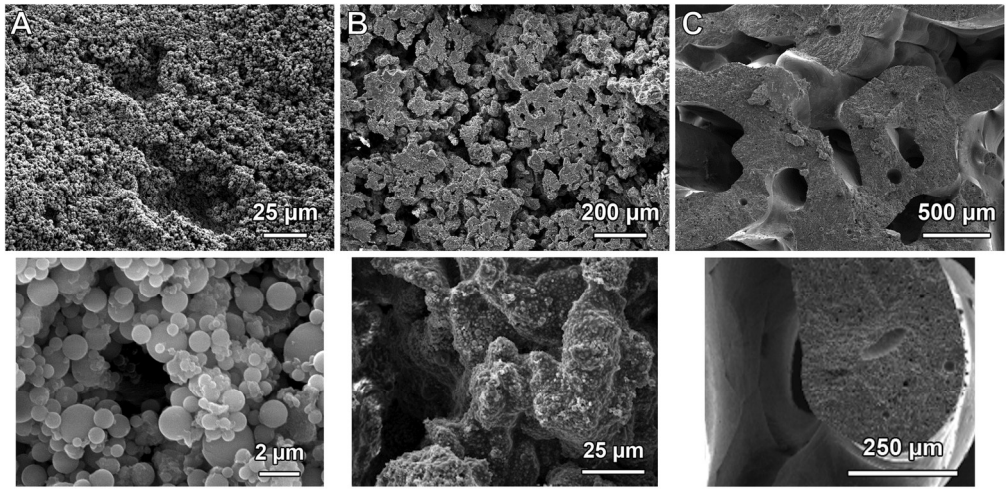

86x41mm (600 x 600 DPI)

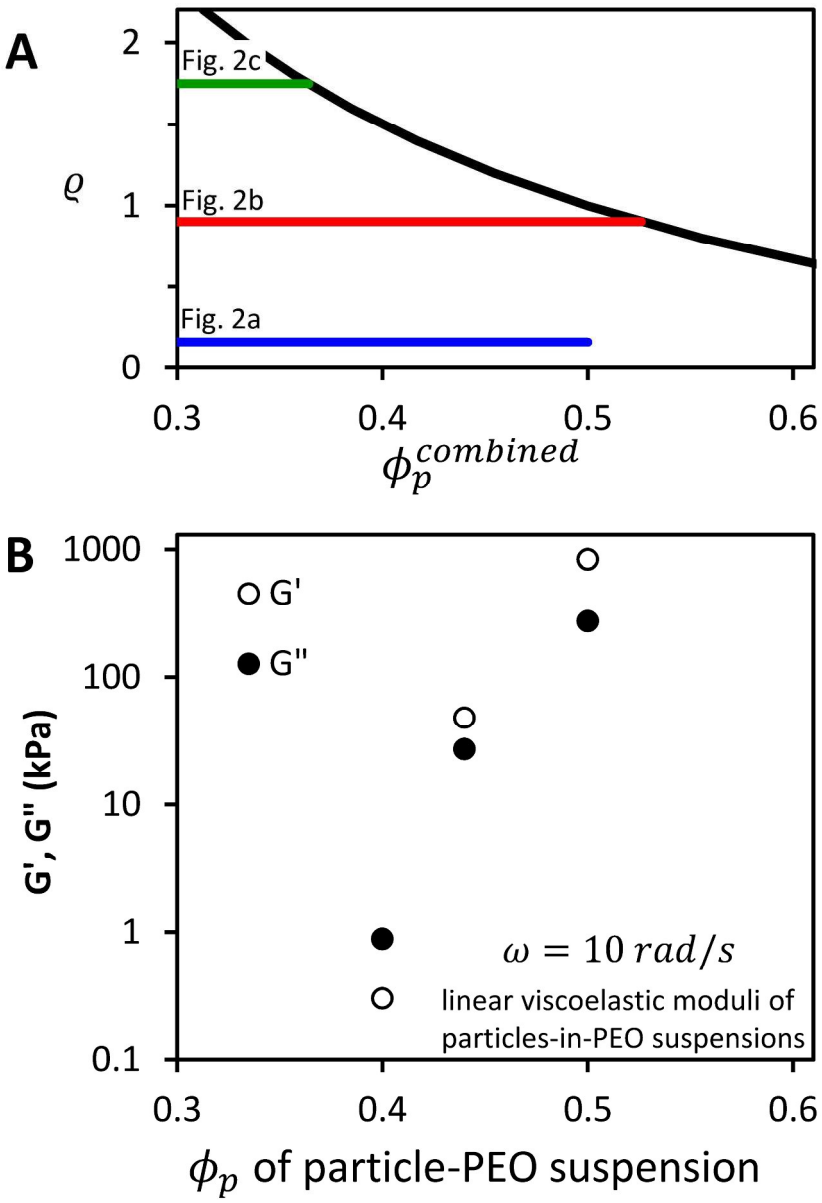

108x159mm (600 x 600 DPI)

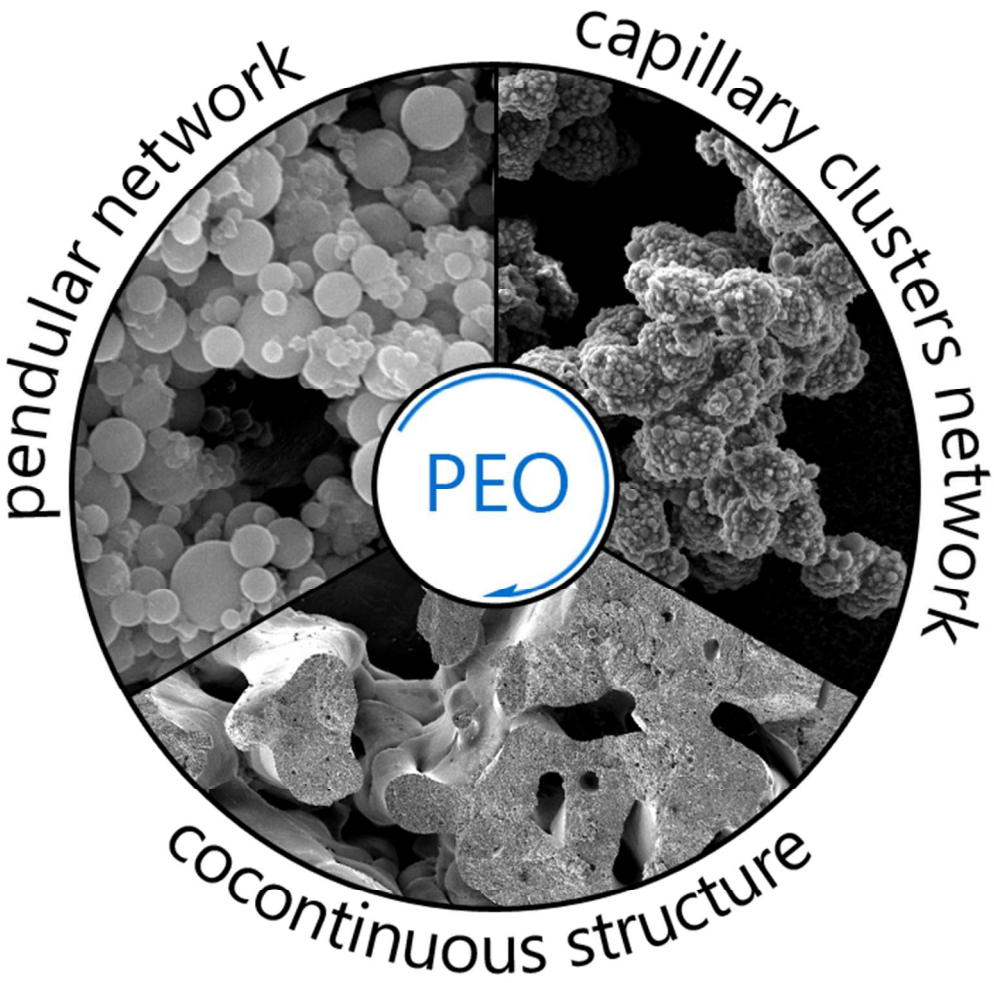

60x60mm (300 x 300 DPI)

Three distinct open-pore morphologies from a single particle-filled polymer blend

Trystan Domenech, Junyi Yang, Samantha Heidlebaugh, Sachin S. Velankar, Dept. of Chemical Engineering, University of Pittsburgh, Pittsburgh PA 15261, USA.*
Phone: (+1) 412-624-9984 ; Email: velankar@pitt.edu

Abstract

Ternary mixtures composed of polyisobutylene (PIB), polyethylene oxide (PEO), and silica particles yield three distinct open-pore morphologies depending on mixture composition: (1) *pendular network* (particles bonded together by menisci of PEO); (2) *capillary aggregate network* (particles and PEO form a combined phase with strongly solid-like properties which percolates); (3) *cocontinuous morphology* (silica and the PEO form a highly viscous combined phase which retards interfacial tension-driven coarsening). Remarkably, interfacial tension plays altogether different roles in stabilizing these three morphologies: stabilizing the first, not affecting the second, and destabilizing the last. The first two of these morphologies appear to be generalizable to other systems, e.g. to oil/water/particle mixtures. In all three cases, the pores do not collapse even after flow, i.e. all three porous morphologies are amenable to processing.

Keywords: rheology; suspension; porous; percolation; ternary mixtures

Introduction

Open pore structures are useful in a wide variety of applications, e.g. absorbing and retaining fluids (e.g. wound dressing, personal hygiene, oil spill absorption), highly compliance structures (e.g. seat cushions), providing percolating pathways (conductive electrodes, battery separator materials, filters, tissue engineering scaffolds). Topologically, open pore structures have two interpenetrating continuous phases, one of which is regarded as "pores" (i.e. typically filled with air or with water), and the other phase being a solid with some mechanical integrity. Open pore structures have diverse morphologies such as networks composed of slim struts (e.g. open-celled foams[1]), interconnected cavities (e.g. polymerized high-internal phase emulsions[2-5]), interstitial spaces between fused particles (e.g. sintered powders[6]) or between fiber mats[7-8], or smooth bicontinuous phases[9-10]. Here we show that a single system composed of two immiscible polymers and one particulate species yields three distinct open-pore morphologies depending on the composition of the mixture.

Experimental

The experimental system is composed of silica particles, and two immiscible polymers, polyethylene oxide (PEO) and polyisobutylene (PIB). Details of the materials are provided in Table 1. All components were mixed together (next paragraph) at 80℃, a temperature at which the PEO and PIB have similar viscosities. Upon cooling to room temperature, the PEO crystallizes into a semicrystalline solid (melting point 65℃); this provides a facile means of quenching the morphology developed under melt-blending conditions. The continuous phase PIB was extracted in octane, leaving behind the consolidated masses of the PEO and the particles discussed below. These were fractured, coated with palladium, and imaged by scanning electron microscopy (SEM).

Being composed of molten polymers, these samples have viscosities far higher than oil/water mixtures. Accordingly they cannot be mixed by simple shaking or by equipment such as a homogenizer. Therefore samples were mixed in a custom-built polymer mixer comprising a rotating disc-cup assembly of 5 ml volume. Three ball bearings were added between the rotating disc and the cup to ensure intensive mixing[11-13]. The cup was maintained at 80℃ using an electric heater. All samples were mixed identically: the minority polymer PEO was first dispersed into the PIB at 1200 rpm, particles were added, and mixing continued for an additional 5 min. Samples were cooled in air immediately after mixing, followed by 30 minutes at ~4℃ to ensure complete crystallization of the PEO.

Results and Discussion

The six different compositions discussed in this article can be placed in a ternary composition diagram[14-15], Fig. S1, from which the volume fractions of all three species can be read off. However for this article, it is more convenient to specify the composition in terms of two parameters: the particle volume fraction, ϕ_p and $\varrho = \phi_{PEO}/\phi_p$, which is the wetting fluid loading relative to the particle loading. This representation is shown in Fig. 1A. Of the six compositions discussed, the three with high values of ϕ_p yield three distinct types of open-pore structures illustrated schematically in Fig. 1B, and discussed below.

Fig. 2A illustrates the first kind of porous structure, dubbed a *pendular network*. This appears when the PEO loading is substantially lower than particle loading, i.e. ϱ is on the order of 0.1, and no larger than 0.3. In this range of ϱ, when the sample is well-mixed, the wetting fluid forms pendular menisci that connect the particles into aggregates. If ϕ_p is small, the pendular aggregates are discrete (Fig. S2). With increasing ϕ_p (at fixed ϱ), these aggregates grow until they percolate, and a pendular network results. Previously we showed that the percolation threshold is only a few percent[12], i.e. the ϕ_p of Fig. 2A far

exceeds the percolation threshold. This pendular network structure is analogous to wet sand in which the sand particles are bridged by menisci of water[16].

Fig. 2B illustrates the second kind of porous structure dubbed a *capillary aggregate network*, which appears when ϱ is 0.5-1. Since the particles are fully-wetted by the PEO, and since the PEO fraction is comparable to the particle fraction, the PEO engulfs the particles completely to form a combined phase. This combined phase is highly concentrated with an internal particle volume fraction of $\phi_p^{combined} = \frac{\phi_p}{\phi_p+\phi_{PEO}} = (1+\varrho)^{-1}$. The dependence of $\phi_p^{combined}$ on ϱ is illustrated in Fig. 3A. For instance, for Fig. 2B, $\varrho = 0.9$, which corresponds to $\phi_p^{combined} = 0.53$. Due to this high particle loading, this combined phase is expected to resemble a paste with solid-like rheological properties. We sought to measure the rheology directly by preparing a particle-in-PEO suspension (no PIB added) at a particle loading of 53 vol%. However we were unsuccessful since the extremely solid-like rheology makes homogeneous mixing difficult. We were however able to prepare particle-in-PEO suspensions with somewhat lower particle loadings and Fig. S4 shows the Large Amplitude Oscillatory Shear (LAOS) rheology of some samples measured at a frequency of 10 rad/s. At 40 vol% particles, G'' exceeds G' over the entire amplitude range, indicative of liquid-like behavior. In contrast at 44 and 50% particles, the rheological behavior is typical of paste-like materials: at low amplitude $G' > G''$, whereas at some larger amplitude, there is a crossover which is often regarded as a signature of yielding. From these data, one may extract the linear viscoelastic moduli of these suspensions (Fig. 3B), and by interpolation, conclude that samples with over ~42% particles have $G' > G''$ indicative solid-like rheology. Thus, a suspension with 53% particles (corresponding to the PEO-phase in Fig. 2B) would be strongly solid-like. Accordingly, when the ternary blend of Fig. 2B is subjected to intense mixing, the combined phase tends to form misshapen "blobs" called *capillary aggregates*[17]. Capillary aggregates tend to be non-spherical since their internal yield stress exceeds their capillary pressure, thus interfacial tension cannot induce a misshapen aggregate to relax into a spherical shape. At low values of ϕ_p these blobs are discrete (Fig. S3), however with increasing ϕ_p, they percolate into the network of Fig. 2B. This network is composed of roughly spherical capillary aggregates which are bonded together through relatively narrow necks[12]. This phenomenon has been documented previously in mixtures of oil, water, and fat where it was called *partial coalescence*[18]. A more evocative term coined by Caggioni et al. is *anisotropic endoskeletal drops*[19], i.e. drops with an internal network that sustains non-spherical shapes. We note that the particles in these previous papers were needle-like crystals[18-19], and hence could develop a yield stress at even low particle loadings. Here, the particles are spherical, and hence anisotropic drop shapes can survive only at high $\phi_p^{combined}$ (low ϱ)

values. Incidentally, the fact that capillary aggregates form at certain compositions is not new[17]; what is unusual is that the capillary aggregates join together into a percolating network.

The third type of porous structure, dubbed a *cocontinuous morphology* (Fig. 2C) is evident at $\varrho = 1.75$. The particles and the PEO still form a combined phase, but now the combined phase is much less crowded than in Fig. 2B. For example, for Fig. 2C, Fig 3A suggests that at $\varrho = 1.75$, the particle volume fraction in the combined phase is 0.36. At this particle loading, the combined phase is highly viscous, but it no longer has significant solid-like properties (indeed even at 40% particles, Fig. S4 indicates liquid-like rheology). Accordingly, particles no longer protrude out from the PEO phase, instead the liquid/liquid interface appears smooth, as typical of systems in which capillarity dominates. Under these conditions, if the combined phase is dilute (Fig. S5), the morphology is composed of spherical drops of PEO with particles incorporated inside. In Fig. 2C in contrast, the combined phase loading is $(\phi_p + \phi_{PEO}) = 0.55$, and a cocontinuous morphology is obtained. Given sufficient time under quiescent conditions after mixing, this system would coarsen indefinitely, and eventually the cocontinuous structure would be destroyed by gravity (there is a significant density difference between the phases due to the high density of silica). Yet, due to the high internal viscosity of the combined phase, coarsening and collapse are relatively slow processes. Thus even air-cooling is sufficiently rapid that the crystallization of PEO can quench the cocontinuous structure readily. It is crucial to note that the particle-free PEO/PIB blends do not form cocontinuous morphologies at *any* PEO:PIB ratio. We have prepared particle-free PEO/PIB blends across a range of compositions and in all cases, the morphology is either a PEO-in-PIB with spherical PEO drops, or vice versa[20]. Thus, the particles are essential to stabilize the cocontinuous morphology. We surmise that the mechanism for such stabilization resembles viscoelastic phase separation[21]: since the combined PEO+particles phase has a high viscosity, interfacial coarsening and breakup, which usually destroy a cocontinuous morhology, are greatly retarded. Incidentally we note that cocontinuous morphologies are commonly reported in the polymer blends literature, even in the absence of particles[9]. In those cases, the polymers being blended have viscosities that are typically 2-3 orders of magnitude higher than those used here. Due to those high viscosities, the morphologies can be quenched readily by cooling.

It is important to note explicitly the major differences between the three morphologies. The pendular network is inherently a particle-scale structure, with the capillary force playing the role of a pair-wise attraction between particles. The percolating network is built from the individual particles bonded together by capillary menisci[16]. The immediate implication is that the pore size is comparable to the particle size, i.e. as long as the network is homogeneous, pore size can be changed only by changing the particle size. In contrast, the capillary aggregate network uses as building blocks not individual particles,

but aggregates comprising a large number of particles, together engulfed by the wetting fluid. Thus the pore size is decoupled from the particle size, and is instead set by the composition (which determines the rheology of the combined particle+PEO phase) and by the mixing conditions (which determines the size of largest capillary aggregate that can survive the mixing process). Finally the pore size of cocontinuous morphology is also decoupled from the particle size. But unlike in capillary aggregates, the combined phase is not internally jammed, and its rheological behavior is liquid-like. Thus this morphology is unstable, and unlike the previous two morphologies, quenching is essential to suppress morphological coarsening. In the present case, quenching is provided by crystallization of PEO, but one may also arrest coarsening by gelation, vitrification, or crosslinking of one or both phases. Since the cocontinuous morphology results from a competition between viscous stress and interfacial tension, we anticipate that the size-scale of the morphology would reduce if the mixing speed were increased although we have not tested this.

It is interesting to note that capillarity (in the sense of minimizing the liquid-liquid interfacial area) plays completely different – indeed opposing – roles in these three cases. In the pendular network, the pairwise attractive force between the particles is attributable to interfacial tension (indeed the meniscus force is proportional to interfacial tension)[22]. Thus the stability of the particle network depends primarily on capillarity; any additional interparticle attractions would confer additional stability. In contrast, the capillary aggregate network is stabilized primarily by the solid-like rheology of the combined particle+PEO phase, and to a first approximation, the stability does not rely on capillarity. In a previous article on oil/water/particle systems[15], we have argued that since particles protrude out of the surface of the capillary aggregates, the liquid/liquid interface has negative curvature, and hence "pulls together" the particles with a Laplace pressure that is on the order of (surface tension)/(particle size). This Laplace pressure increases the interparticle friction forces, and may therefore increase the yield stress within the capillary aggregates. To the extent that this mechanism is active, capillarity may have a stabilizing effect on the capillary aggregate network. Finally, in the cocontinuous morphology, capillarity induces morphological coarsening as well as breakup into a droplet-matrix morphology. Thus in this case, capillarity has a *de*stabilizing effect. It is for this reason that the cocontinuous structure *must* be quenched, whereas the pendular or capillary aggregate networks need not be.

It is of immediate interest to ask whether these three morphologies are unique to polymeric mixtures, or if they may be realized even when the fluids are oil and water. The pendular network is highly general and can be realized in almost any particulate system in which the particles are preferentially-wetted by the minority phase. For instance, Fig. S6 illustrates a pendular network realized from large glass particles, but using oil as the continuous phase and water as the dispersed phase that forms the meniscus. With

hydrophobic particles, one may also realize an inverted structure in which water is continuous and oil is the meniscus-forming phase. The capillary aggregate network also appears to be generalizable to oil/water systems. For instance, Figs. S7A&B show a network formed by using the same particles as used in the rest of this paper, but with oil and water as the two fluids. The sample was mixed using a high speed rotor-stator mixer using the procedure described in the caption to Fig. S7. A network of capillary aggregates is clearly evident at $\varrho = 0.75$. The same procedure was applied using polyethylene particles, methanol and a small quantity of mineral oil (see caption of Fig. S8 for compositions). Since the polyethylene particles are highly oleophilic, a capillary aggregate network with methanol as the continuous phase was realized. Finally, we were unsuccessful in realizing cocontinuous morphologies from oil/water systems. For instance, Fig. S7A&B show capillary aggregates realized in an oil/water system at $\varrho = 0.75$. Upon increasing the ϱ to 0.8, the capillary aggregates become capable of complete coalescence indicative of increasingly liquid-like behavior of the (silica+water) combined phase. But instead of realizing a cocontinuous morphology, Fig. S7C shows that the system collapses into separated mixture of oil and (silica+water). Thus even if the cocontinous morphology was present during mixing, it does not survive for any significant duration after mixing. We believe that this rapid collapse is attributable to the much lower fluid viscosity of the oil/water system as compared to the PEO/PIB blends. Thus, as already emphasized above, the cocontinuous morphology can be realized only if at least one of the fluid phases can be solidified rapidly. In summary, at least two of the three morphologies appear to be generalizable to oil/water systems; whereas the last, the cocontinuous structure, is not.

We have not investigated in detail the boundaries separating these three porous structures. A review across a wide range of systems suggests that the pendular aggregate morphology becomes unstable when menisci binding different particles start coalescing together[14]. This happens at $\rho \sim 0.35 - 0.5$, which may be taken as the boundary separating a pendular network from capillary aggregate network. The boundary between capillary aggregates and cocontinuity (if cocontinuity is realized) depends on the ϱ value above which the combined phase has liquid-like rheology. This boundary is more difficult to generalize across a wide range of systems; depending on the nature of particle interactions, some combined phases may become solid-like at even relatively high ϱ values. Indeed, some previous researchers have reported stabilization of cocontinuous-like morphologies in polymeric systems even at very low particle loading[23-25] because the nanoparticles were able to induce solid-like rheology even at low particle loading.

Conclusions and Outlook

In summary, we show that by changing composition, a single three-component mixture yields three porous morphologies that have distinct size-scale and entirely different mechanisms of structural

stabilization. What is most remarkable is interfacial tension plays an altogether different role, stabilizing the pendular morphology, destabilizing the cocontinuous morphology, and (to a first approximation) not affecting the capillary aggregate network. At least two of these porous structures appear to be generalizable to other mixtures, including to oil/water/particle mixtures. Two noteworthy aspects that are relevant to practical applications must be emphasized. First, in all three of the porous structures reported here, both phases are continuous, i.e. they may be regarded as open-pore structures with potential applications listed in the first paragraph of this article. The resulting porous structures may be used directly, e.g. for tissue scaffolds. Alternately, one may remove the non-wetting fluid by selective extraction (as done here), drying, or simply draining out the fluid, and then undertake further modifications, e.g. particle sintering, back-filling the pores with other fluids, etc. Indeed particulate networks based on capillary attractions have already been used to fabricate porous ceramics[26-27]. Second, all three of these structures were generated under flow conditions, and longer flow duration under molten conditions does not disrupt them. Thus, as long as the yield stress is not too high (which may happen at higher particle loadings), these morphologies are all amenable to be molded, extruded, or injected – without losing their open pore morphology. This is in contrast to many other methods of fabricating similar open-cell porous structures, e.g. polymerizing a high internal phase emulsion, preparing a bijel precursor[10], leaching a porogen[28], phase separation of a polymer solution, or direct foaming of polyurethanes. In all those cases, open-celled porous structure cannot be subjected to flow, either because it is quenched, or because it does not survive under flow.

Acknowledgements: We gratefully acknowledge the National Science Foundation for financial support (NSF-CBET grant no. 0932901 and 1336311), Samantha Heidlebaugh (Figs. S6 and S7) and Dr. Manjulata Singh and Prof. Shilpa Sant (Figs. S6b) respectively. Fig. S1 was drawn using the ternary diagram template provided by Graham and Midgley[29].

References

1. Defonseka, C., *Practical Guide to Flexible Polyurethane Foams*. Smithers Rapra Technology: **2013**.
2. Haibach, K.; Menner, A.; Powell, R.; Bismarck, A., Tailoring mechanical properties of highly porous polymer foams: Silica particle reinforced polymer foams via emulsion templating. *Polymer* **2006,** *47* (13), 4513-4519.
3. Barbetta, A.; Rizzitelli, G.; Bedini, R.; Pecci, R.; Dentini, M., Porous gelatin hydrogels by gas-in-liquid foam templating. *Soft Matter* **2010,** *6* (8), 1785-1792.
4. Foudazi, R.; Gokun, P.; Feke, D. L.; Rowan, S. J.; Manas-Zloczower, I., Chemorheology of Poly(high internal phase emulsions). *Macromolecules* **2013,** *46* (13), 5393-5396.
5. Silverstein, M. S., Emulsion-templated porous polymers: A retrospective perspective. *Polymer* **2014,** *55* (1), 304-320.

6. Liu, P. S.; Chen, G. F., *Porous Materials: Processing and Applications*. Butterworth-Heineman: Oxford, **2014**.
7. Masoodi, R.; Pillai, K., *Wicking in Porous Materials: Traditional and Modern Modeling Approaches*. CRC Press: Boca Raton, **2013**.
8. Ding, B.; Yu, J., *Electrospun Nanofibers for Energy and Environmental Applications*. Springer: Heidelberg, **2014**.
9. Potschke, P.; Paul, D. R., Formation of Co-continuous structures in melt-mixed immiscible polymer blends. *J. Macromol. Sci.-Polym. Rev* **2003,** *C43* (1), 87-141.
10. Lee, M. N.; Mohraz, A., Bicontinuous Macroporous Materials from Bijel Templates. *Adv. Mat.* **2010,** *22* (43), 4836-4841.
11. Maric, M.; Macosko, C. W., Improving polymer blend dispersions in mini-mixers. *Polym. Eng. Sci.* **2001,** *41* (1), 118-130.
12. Domenech, T.; Velankar, S. S., On the rheology of pendular gels and morphological developments in paste-like ternary systems based on capillary attraction. *Soft Matter* **2015,** *11* (8), 1500-16.
13. Domenech, T.; Velankar, S., Capillary-driven percolating networks in ternary blends of immiscible polymers and silica particles. *Rheol. Acta* **2014,** *53* (8), 1-13.
14. Velankar, S. S., A non-equilibrium state diagram for liquid/fluid/particle mixtures. *Soft Matter* **2015,** *11* (43), 8393-8403.
15. Heidlebaugh, S. J.; Domenech, T.; Iasella, S. V.; Velankar, S. S., Aggregation and Separation in Ternary Particle/Oil/Water Systems with Fully Wettable Particles. *Langmuir* **2014,** *30* (1), 63-74.
16. Herminghaus, S., Dynamics of wet granular matter. *Adv. Phys.* **2005,** *54* (3), 221-261.
17. Pietsch, W., Chapter 7: Tumble/growth agglomeration. In *Agglomeration Processes: Phenomena, Technologies, Equipment*, Wiley: Weinheim, **2008**.
18. Boode, K.; Walstra, P., Partial Coalescence in Oil-in-Water Emulsions .1. Nature of the Aggregation. *Colloid Surf. A* **1993,** *81*, 121-137.
19. Caggioni, M.; Bayles, A. V.; Lenis, J.; Furst, E. M.; Spicer, P. T., Interfacial stability and shape change of anisotropic endoskeleton droplets. *Soft Matter* **2014,** *10* (38), 7647-7652.
20. Domenech, T.; Velankar, S. S., Microstructure and phase inversion in three phase polymer/polymer/particle blends. *In preparation.* **2015**.
21. Tanaka, H., Viscoelastic phase separation. *J. Phys.-Condes. Matter* **2000,** *12* (15), R207-R264.
22. Willet, C. D.; Johnson, S. A.; Adams, M. J.; Seville, J. P. K., Chapter 28: Pendular capillary bridges. In *Handbook of powder technology, Vol. 11, Granulation*, Salman, A. D.; Hounslow, M.; Seville, J. P. K., Eds. Elsevier: Amsterdam, **2007**.
23. Cai, X. X.; Li, B. P.; Pan, Y.; Wu, G. Z., Morphology evolution of immiscible polymer blends as directed by nanoparticle self-agglomeration. *Polymer* **2012,** *53* (1), 259-266.
24. Khademzadeh Yeganeh, J.; Goharpey, F.; Moghimi, E.; Petekidis, G.; Foudazi, R., Manipulating the kinetics and mechanism of phase separation in dynamically asymmetric LCST blends by nanoparticles. *PCCP* **2015,** *17* (41), 27446-27461.
25. Wu, G.; Li, B.; Jiang, J., Carbon black self-networking induced co-continuity of immiscible polymer blends. *Polymer* **2010,** *51* (9), 2077-2083.
26. Dittmann, J.; Koos, E.; Willenbacher, N., Ceramic Capillary Suspensions: Novel Processing Route for Macroporous Ceramic Materials. *J. Am. Ceramic Soc.* **2013,** *96* (2), 391-397.

27. Koos, E.; Willenbacher, N., Capillary Forces in Suspension Rheology. *Science* **2011,** *331* (6019), 897-900.
28. Tessmar, J. K. V.; Holland, T. A.; Mikos, A. G., Salt leaching for polymer scaffolds: Laboratory-scale manufacture of cell carriers. In *Scaffolding in tissue engineering*, Ma, P. X.; Elisseeff, J., Eds. CRC Press: Boca Raton, **2006**.
29. Graham, D. J.; Midgley, N. G., Graphical representation of particle shape using triangular diagrams: An Excel spreadsheet method. *Earth Surface Processes and Landforms* **2000,** *25* (13), 1473-1477.

Table 1

	viscosity (80°C)	**MW**	**Supplier**
polyethylene oxide (PEO)	13 Pa.s	20 kg/mol	Fluka
polyisobutylene (PIB)	8 Pa.s	2400 g/mol	Soltex
silica average ~2 μm diameter			Industrial Powder

List of figures

Fig. 1: (A) Compositions of the samples discussed in the article. The same compositions are represented within a ternary composition diagram in Fig. S1. (B) Idealized illustrations of the three different types of porous structures corresponding to the compositions indicated by the arrows.

Fig. 2: (A) Pendular network (B) Capillary aggregate network; (C) Cocontinuous morphology. Images in the lower row are the same samples as the upper row, but at higher magnification.

Fig. 3: (A): The function $\phi_p^{combined} = (1 + \varrho)^{-1}$, corresponding to the particle volume fraction in the PEO-phase of a PIB/PEO/particle blend. The three horizontal lines correspond to the ϱ values of the three porous structures of Fig. 2. (B) Linear viscoelastic moduli G' and G" of suspensions of particles in PEO.

This is a low resolution version. Higher resolution TIF image has been uploaded separately.

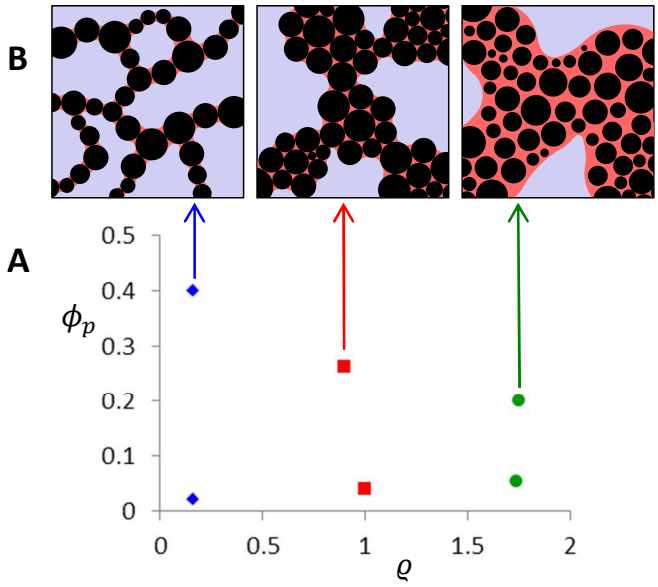

Fig. 1: (A) Compositions of the samples discussed in the article. The same compositions are represented within a ternary composition diagram in Fig. S1. (B) Idealized illustrations of the three different types of porous structures corresponding to the compositions indicated by the arrows.

This is a low resolution version. Higher resolution TIF image has been uploaded separately.

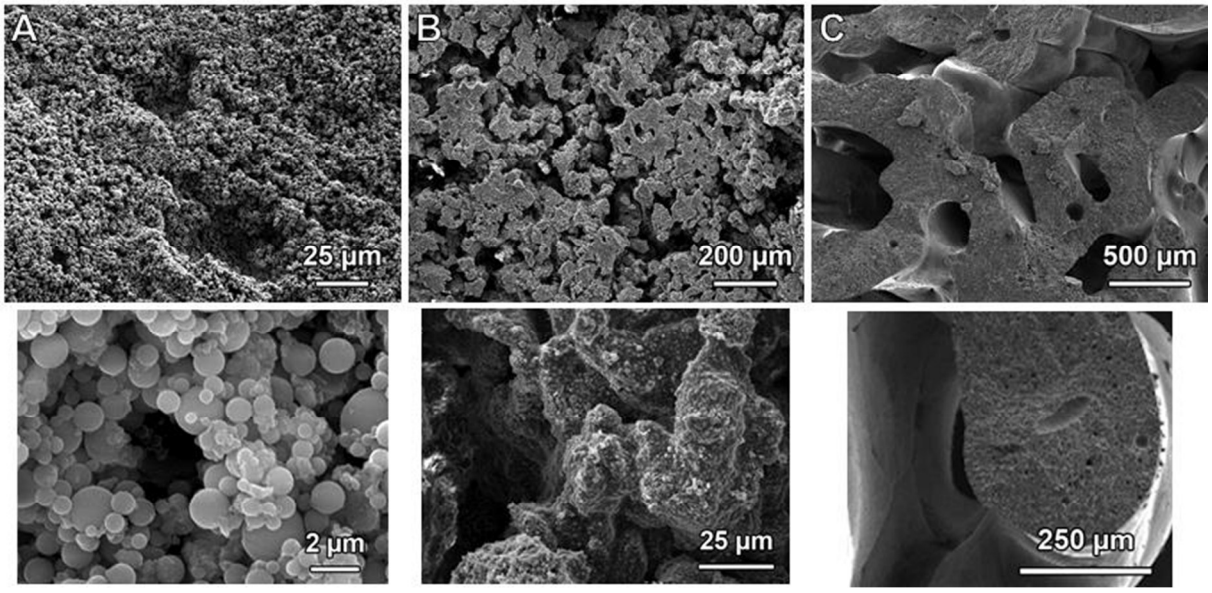

Fig. 2: (A) Pendular network (B) Capillary aggregate network; (C) Cocontinuous morphology. Images in the lower row are the same samples as the upper row, but at higher magnification.

This is a low resolution version. Higher resolution TIF image has been uploaded separately.

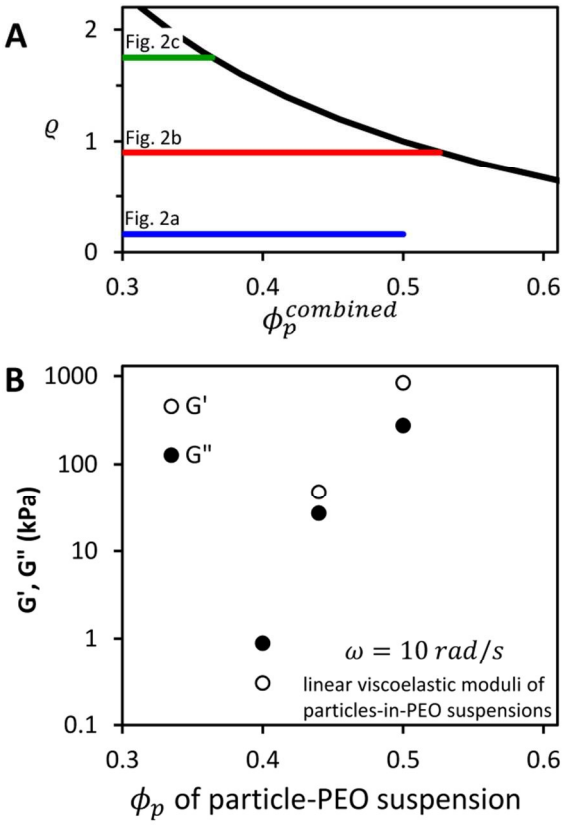

Fig. 3: (A): The function $\phi_p^{combined} = (1 + \varrho)^{-1}$, corresponding to the particle volume fraction in the PEO-phase of a PIB/PEO/particle blend. The three horizontal lines correspond to the ϱ values of the three porous structures of Fig. 2. (B) Linear viscoelastic moduli G' and G" of suspensions of particles in PEO.